QUANTITATIVE ANALYSIS OF NIP-INDUCED TENSION BY USE OF DIGITAL IMAGE PROCESSING

by

B. Gueldenberg and E. G. Welp
Ruhr-University Bochum
GERMANY

ABSTRACT

Winding paper in contact with a drum leads to the production of nip-induced tension which, to a high degree, influences the structure of the roll. Thus, comprehending the processes in the nip, including each parameter involved, is desirable to avoid roll defects.

This paper deals with a new measurement technique that is able to observe the process of building up nip-induced tension in the outer layers of a roll. With the use of digital image processing, this method ensures the registration of the two-dimensional displacement field of the outer layers with fairly high precision. Based on the first principal of the equations of mechanics, it is possible to derive the stress and strain in the layers from the displacement field. Thus, it succeeds to calculate the tangential stress in the outer layers of a roll taking the compression as well as the slippage of the layers into account.

In all experimental test series the tangential stress increases within the first 4 to 15 layers to a maximum value. Afterwards, there is still a considerable displacement of the layers relative to the core, but the layer-to-layer slippage is so small that the change in strain is negligible. Furthermore, it is shown that there is a reduced increase of nip-induced tension in the first approximate 50 layers near the core. Comparing the nip-induced displacement of different type of papers, there are clearly differences noticeable concerning the amount of displacement, as well as the rapidness of increase to the final displacement.

NOMENCLATURE

E	Youngs modulus
h	thickness of the web
i	number of the observed layer

j number of outer layers relative to layer i
N number of outermost layer
r radius
T tension, load [N/cm]
u displacement
δ change of the following parameter due to a newly wound on layer
Δ difference of the following
ε strain
μ coefficient of friction
ν Poisson's ratio
σ web stress

Indices
a axial
(corresponds to the cross direction (CD) of the paper)
E incoming paper
H stick
G slip
N nip
n normal direction
r radial direction
(corresponds to the z- direction (ZD) of the paper)
t tangential direction
(corresponds to the machine direction (MD) of the paper)

INTRODUCTION

Purpose

Surface winders are widely used in paper producing and converting industry as two drum winders, single drum winders or pope reel. A characteristic of all types of winders is that the process inside the nip essentially influences the state of tension and strain in the roll. It is known that a large part of all roll defects are caused by a nip effect that is either to strong (e.g. internal web break in MD), to soft (e.g. telescoped rolls) or a nonuniform nip effect (e.g. cross machine wrinkles) [1,2]. There are various parameters influencing the process inside the nip and the mutual dependences of these parameters are numerous. This makes it difficult to have a fundamental understanding of the the winding process and the consequences of changing a winding parameter is often unpredictable. These problems are increasing due to the production of bigger roll diameters and widths as well as to new paper grades. The limits of todays winding technology are obviously reached. A purposeful and effective developement of the machine technology and a reliable control of the winding process is only possible with a solid basis of fundamental knowledge. Thus, comprehending the process in the nip, including the influence of each parameter involved, is desirable to avoid roll defects at present and in future.

Background

Todays winding models use a ring approximation for each layer of the roll instead of the spiral design of the roll. The two boundary conditions required to solve the second order differential equation are the stiffness of the core and the tangential stress σ_{tE} of the incoming web. The winding models are able to precisely calculate the radial and tangential stresses inside a wound roll for center winders whereas there are major differences in the calculated and existing stresses in the case of surface winders due to the nip-induced tension which is not taken into account.

According to current investigation of nip mechanics, the nip-induced tension is built-up in the outer layer of a roll when passing the nip. Pfeiffer [3] explains this mechanism with the existence of an instant center beneath the surface of the roll. Good and Wu [4] find out that the mechanism responsible for the nip-induced tension is an elongating MD strain caused by the Poisson's ratio and compressive stresses in CD and ZD. In [5] the nip mechanics are investigated for the case of a single web wrapping a rigid roll in combination with a Hertzian pressure distribution. It is shown that the influence of Poisson's ratio due to the Hertzian pressure distribution leads to stress changes in MD which can be identified as slip zones. However, the model is restriced to a single layer in a nip. Resuming it can be stated, that a sufficient description of the process inside the nip by means of analytical equations does not exist, so a calculation of the nip-induced tension based on the first principal equations including material parameters and process parameters is not possible at this time.

First quantifications of nip-induced tension were achieved experimentally. The nip-induced tension was measured as the difference of the tangential stress in a web before and after the nip, whereby the boundary conditions of the real winding process were reconstructed with different accuracy. Reference is made to the first investigations of Pfeiffer [3], which were continued later by the development of different sophisticated trial stands [6,7]. Furthermore Rand and Eriksson [8] observed the progression of the tangential stress in the paper on a two drum winder by means of a strain gauge which was fixed on the paper.

Apart from measuring stress, the tension producing mechanism of the nip was studied indirectly by observing the displacement of paper layers inside the roll. The nip effect causes layer-to-layer slippage, which becomes apparent by means of the so-called J-lines [9]. The repeated application of J-line measurements and the connection of the end point of J-lines afterwards, leads to a curve which describes the final displacement of each layer at the end of the winding process [10].

However, because of the macroscopic observation of the layers displacement field, a quantitative derivation of the nip-induced tension from the observed displacement field is not possible. The tension producing mechanism is limited to the outer 5 to 15 layers, where one can observe considerable displacement towards the direction of rotation [10,11]. This motion corresponds to a closing of the winding spiral and consequently increases the tangential stress in the web. As this part of the winding spiral differs clearly from the rest of the spiral, it shall be called "**active spiral**".

Methods

This paper presents a new measurement technique to determine the nip-induced tension in the active spiral. For this purpose the two-dimensional displacement field of the outer layers is registered by use of digital image processing. In addition the relation between the displacement field and the strain and stress in tangential direction is derived, because we do not directly investigate the nip-induced tension.

RELATION BETWEEN LAYER DISPLACEMENT AND NIP-INDUCED TENSION

If one assumes plane deformation, the relations between stress and strain for an orthotropic material is given by:

$$\varepsilon_t = \frac{1-\nu_{ta}\cdot\nu_{at}}{E_t}\cdot\sigma_t - \frac{\nu_{tr}-\nu_{ta}\cdot\nu_{ar}}{E_r}\cdot\sigma_r$$

$$\varepsilon_r = \frac{1-\nu_{ra}\cdot\nu_{ar}}{E_r}\cdot\sigma_r - \frac{\nu_{rt}-\nu_{ra}\cdot\nu_{at}}{E_t}\cdot\sigma_t$$

$$\varepsilon_a = 0 \qquad (1)$$

The tangential stress σ_t of the web changes during the winding process depending on:

- the position inside the roll described by the variable i ,
- the distance from the outer radius described by the variable j (see Fig. 1).

The tangential stress can be expressed as a function of i and j as follows:

$$\sigma_t(i,j) = \sigma_{tE} + \Delta\sigma_t(i,j) \qquad (2)$$

whereas the term σ_{tE} corresponds to the stress of the incoming web and the term $\Delta\sigma_t$ refers to the change of stress during the winding process. Considering that paper has a small Poisson's ratio in ZD and that the following investigations concentrate on the outer layers of the roll where the radial stress is small compared to the tangential stress, we obtain for the relation between tangential stress and strain according to (1) and (2):

$$\varepsilon_t(i,j) = \varepsilon_{tE} + \Delta\varepsilon_t(i,j) = \frac{\sigma_{tE}+\Delta\sigma_t(i,j)}{E_t} \qquad (3)$$

The change of the tangential strain $\Delta\varepsilon_t$ is, according to Fig. 2, again depending on the displacements u_r and u_t. As an extension to the winding models based on concentric rings, the spiral structure of the roll is taken into account by consideration of the tangential displacement. In this manner, the stress increasing influence of the nip-induced layer displacement can be considered. The additional existing local deformation of the roll in the nip zone is not taken into account in this paper. We get for $\Delta\varepsilon_t$:

$$\Delta\varepsilon_t = \Delta\varepsilon_{t,u_r} + \Delta\varepsilon_{t,u_t} = \frac{u_r}{r} + \frac{\Delta u_t}{2\pi\cdot r} \qquad (4)$$

The **radial displacement** u_r is the sum of the compressions of all inner layers due to the radial compressive stress of the outer layers. It can be calculated by means of a winding model. The radial displacements are directed to the core ($u_r < 0$). They are responsible for the well-known decrease of the tangential stress inside the roll.

The **tangential displacement** Δu_t describes the relative motion of two layer marks which isolate a single layer. In the outer layers the tangential displacement is directed towards the direction of rotation of the roll and therefore contributes to a stress increase, generally known as the nip-induced stress.

When regarding the development of the total tangential stress in the active spiral, one must consequently consider the reduction of stress caused by the compression of the paper layers and the increase of stress due to the layer-to-layer-slippage. From the displacement field u_r, u_t both parts can be derived according to the equations (2)-(4).

Radial displacements during the winding process

Winding on a single lap, causes an increase of the radial compressive stress $\delta\sigma_r$ inside the roll (see Fig. 3). This stress increase causes an additional compression, i.e. a reduction of thickness δh of all inner layers. By double summing δh over all inner layers i and all added layers j, the total radial displacement u_r can be written as:

$$u_r(i,j) = \sum_j \sum_i h \cdot \frac{\delta\sigma_r}{E_r} \tag{5}$$

In Fig. 4 one can see the radial displacement calculated on the basis of Hakiel's winding model as a function of the layer number i for different outer radius N. It is obvious, that the radial displacement increases very quickly from 0 at the outside of the roll to its maximum value after winding on approximately 100 to 300 layers depending on the distance from the core. After reaching this maximum value the radial displacement does not change any more when the winding process is continued. The rapid increase of the radial displacement in the active spiral is caused by the great increase of the radial stress $\delta\sigma_r$ and the small Youngs-modulus E_r in the outer layers of a roll.

We performed calculations based on Hakiel's winding model to approximate the total radial displacement expected in the activ spiral during our trials. Five different paper grades covering the whole spectrum of printing papers were used. The corresponding material properties are listed in Table 1. The total radial displacement after winding on 15 layers was calculated for all different paper grades, for two different web tensions (T_E=1,5 bzw. 5,5 N/cm) and different distances from the core (i=50, 100, 200, 500, 1000). The results are shown in Table 2 and can be summarized as follows:

- The radial displacement is always less than 70 μm.
- Higher thickness of the paper and lower resistance in ZD results in a higher radial displacement.
- Higher web tension of the incoming web results in a higher radial displacement.
- The influence of the position in the roll on the radial displacement is very small.

Tangential displacements during the winding process

The tangential displacement δu_t shall be the displacement of a layer mark in circumferential direction relative to a reference mark on the core caused by winding on a single layer j (see Fig. 5). To calculate the tangential strain of the layer, the total displacement is not important, but the difference of the tangential displacement $\Delta\delta u_t$ of two layer marks isolating a single layer is. If one sums $\Delta\delta u_t$ over all layers wound on, it follows:

$$\Delta u_t(i, j) = \sum_j [\delta u_t(i) - \delta u_t(i-1)] \tag{6}$$

Looking at the total layer displacement by means of the J-lines already mentioned, one can recognize total displacements of a few centimeters at the J-lines' endpoints. However, the differences of the total displacements of two layer marks isolating a single layer are very small. Consequently, the changes of strain are insignificantly small. Only if gaps can be clearly seen between two marks, the intermediate layer is subject to an essential changing of strain. Such tangential differences of displacement only occur in the outer 5 to 15 layers as one can conclude from the following experimental investigations.

EXPERIMENTAL INVESTIGATIONS

Description of the experimental winder

The experimental investigations were performed on an experimental winding line, which simulates the winding process on a single drum winder. Fig. 6 shows the details of this winding line. Only the drum (a) is driven. The core and the tight inner part of the roll is simulated by a steel roll (b) guided by poles (c). It moves vertically when the radius of the roll increases. The web tension and the nip load are available to control the increase of roll tightness. The web tension is controlled by an adjustable brake and recorded by a measuring roll (d) before entering the drum. The nip load can be influenced by the counterweight (e). The web width is 120 mm. The rotation angle of the roll is registered by an incremental rotary encoder (f). Each time the roll completes a full rotation, the edge of the paper is marked by an ink-jet printer (g) just before the paper enters the nip and the camera (h) captures a picture precisely at the moment when the marks pass by. In this manner one picture is taken at each turn of the roll.

The integrated measurement instrumentation assumes the following tasks (see Fig. 7):

- aquisition: - angle of rotation of the roll
  - web tension
  - digital image
- control: - printing of layer marks
  - asynchronous shuttering of the camera
- processing: - motion analysis

The whole instrumentation is based on an PentiumII-computer in connection with three boards: a Multi-I/O-board, a Timer/Counter-board and a Frame-Grabber-board. All programming work concerning the aquisition, control and processing was done in LabVIEW, a graphical programming language.

Digital image aquisition

Special attention is drawn to the image aquisition, as it essentially contributes to the accuracy of the system. With a digital point of view, an image corresponds to an array of data, whose values are between 0 (=black) and 255 (=white). The aim of the image aquisition is to capture, on request, the gray scale distribution of a picture and to save it in a format appropriate for further digital processing. This procedure can not be realized with sufficient accuracy by conventional video cameras. In case of moving objects (dynamic imaging) there are some special requirements which have to be fulfilled:

- progressive scan,
  i. e. capturing the picture information simultaneously on all CCD-Sensors in a single shutter event instead of breaking the integration period into two sequentiell field scans with half the resolution each (interlaced mode),
- synchronous pixel clocking,
  i.e synchronizing the D/A sampling of the camera with the A/D sampling of the frame grabber by means of the transfer of the synchronization signals separated from the video signal,
- asynchronous shuttering,
  i.e. electronic shuttering on a triggered event by use of an asynchronous digital control signal

The aforementioned image aquisition system consists of an M10BX progressive scan camera of JAI connected to a IMAQ-1408 frame grabber board of National Instruments and meets the requirements mentioned. The camera has a 8 bit CCD sensor consisting of 782x582 pixel.

Thus, the accuracy of the image aquisition is guaranteed in the range of one pixel. Depending on the adjusted aperture ratio of the used zoom lens one pixel corresponds to a distance of 2,5 to 40 μm, which is the accuracy to determine the location of objects when processing the images.

Digital image processing

The purpose of the digital image processing is to determine the two-dimensional displacement field of the observed objects in an image relative to a reference image. First, the observed objects (here: the marks on the edge of the layers) have to be identified and their location in relation to a reference mark has to be determined. By comparing the location of the identified marks in the two images, the displacement vectors can be calculated.

This process is divided into the following steps (see Fig. 8):

1. Conversion of the gray scale image into a binary image by the use of a threshold function.
2. Application of different morphology functions (low pass, high pass,) to eliminate undesirable objects.
3. Application of a labelling function to identify separated objects.
4. Object measurement to determine the coordinates of the center of gravity and to calculate characteristics of the objects (object area, perimeter, ...)
5. Assignment of identical objects in the two images based on the object characteristics and calculation of the displacement vector.

Sometimes the last step is critical because the marks on the layers are changing their characteristics during the winding process due to the compression of the layers or variation of illumination. If these changes exceed a certain extent, the automatic assignment is no longer successful and a manuel correction is necessary.

After determing the displacement field the appropiate stress and strain can be calculated using equations (2-4).

EXPERIMENTAL RESULTS

Total layer displacement in a roll

Fig. 9 shows the total layer displacement (a) of the outer 300 layers of a roll. As already mentioned, the marks are always printed on the paper edge just before the nip when the roll has completed a full revolution. So, in the case of no layer displacements there will be an almost radial line (b) in the roll (=reference line). Due to the increasing radius of the roll in conjunction with the constant distance between printer and nip this line inclines slightly to the direction of rotation. The relative distance of a layer mark to the reference line corresponds exactly to the total tangential displacement of the layer since it is wound on the roll. In contrast to this method, the well-known J-lines only make the layer displacements visible which occur after the the J-line is printed on the roll. The layer displacements of the inner layers already completed at that time, are not considered. Thus only the displacement of the present outer layer is recorded completely. Hence, only the endpoints of the J-lines (c), as shown in Fig.9, coincide with the graph of the total displacements (a).

The graph of the total displacements intersect the reference line at a the point (d) and can be divided in an inner section where the marks are moved in the direction of rotation and an outer section where the marks are moved towards the direction of rotation. Furthermore a gap between the marks of the outmost layers can be noticed, indicating excessive tangential displacements.

Change of strain and stress due to radial displacements in the active spiral

The pictures taken by the camera correspond to a surface of approx. 6x8 mm, so one pixel corresponds to a distance of 10,4 µm. The measured radial displacements of the tested paper grades are to be found next to the accuracy of the measuring system, which leads to a great dispersion of the measured values. Nevertheless, one can notice a qualitative correlation between the experimental and theoretical values. Comparing the experimental values of Table 3 with the theoretical values of Table 2, it is seen that on the one hand there is a congruence of the order of magnitude. On the other hand, the differences in radial displacement comparing the paper grades show the same tendencies in both tables. As expected the highest radial displacement for newsprint. Fig.10 shows additionally the experimental values of the radial displacement u_r as a function of wound-on layers. These results of 13 observed layer marks are shown as their average value and span in comparison to the values calculated on the basis of the Hakiel model. The curves show the same qualitative development, i.e. increasing radial displacement with increasing outer radius. On the basis of the radial displacements one can calculate the reduction of tangential stress according to equation (2-4). These results are also shown in Table 3.

Change of strain and stress due to tangential displacements in the active spiral

Fig. 11 shows the displacement δu_t of a layer mark as a function of j, the number of added layers or nip passages. A negative displacement δu_t corresponds to a displacement towards the direction of rotation. After the first 9 nip passages δu_t changes the algebraic sign and indicates that a maximum value of total displacement towards the direction of rotation is reached (see point (e) in Fig. 9). Continuing the winding process, the layer marks starts moving to the direction of rotation.

The difference of the displacement of two layer marks $\Delta\delta u_t$ is essential to calculate the layer strain, as already explained in Fig. 5. From the mathematical point of view, this corresponds to the derivation of δu_t. This graph is also shown in Fig. 10. As long as

$\Delta\delta u_t > 0$, the difference of total displacement Δu_t increases and according to equations (2-4) consequently the tangential stress and strain increase too. The decisive factor, if the stress and strain increase or decrease in a layer, is not the direction of displacement of the two layer marks isolating this layer, but the difference of the displacement. Even both marks move towards the roll's direction of rotation, there is an increase of strain in the intermediate layer provided that the mark being closer to the core moves more than the outer one.

Total tangential stress in the active spiral of a roll

In Fig. 12 one can see the development of the total tangential stress according to equation (2) and considering the effect of layer compression ($\Delta\sigma_{t,\,u_r}$) and slippage ($\Delta\sigma_{t,\,u_t}$). Pay attention to the logarithmic scale of the of the x-coordinate. Initially the stress increase due to the nip-induced layer slippage far exceeds the stress reduction due to the layer compression. After about 9 layers counted from the outside of the roll towards the core, the total tangential stress reaches its maximum. This stress maximum inside the roll correlates with the existence of machine direction bursts, known as internal web break, which occur slightly under the surface of the roll in case of excessive nip load and web tension. After the stress maximum, the tension producing effect of the nip looses importance so that the effect of compression is dominating. The total tangential stress starts to decrease and progresses towards zero or even to a slightly compressive stress, as it is already well known from the calculations of the winding models.

Development of nip-induced tension near the core

During one experimental series with fixed settings for nip load and web tension extending over 100 new wound layers, one could not see any essential dependence between the displacement and the position in the roll. After a change in the settings the resulting effect on the displacement could be immediately observed.

In contrast to this, the situation near the core is different. In Fig. 13 you can see the development of the nip-induced displacement Δu_t for different distances from the core described by the layer number i. At the beginning of the winding a tension producing mechanism is not detected. With increasing distance from the core, the observed layer displacement starts to increase to the final value which is reached after about 50 layers. This observation coincides with the fact, that only high web tension and an additional differential moment can help to wind up a strong roll tightness at the beginning of the winding process. Even the application of excessive nip forces will not have a major tension producing effect in the layers close to the core.

Nip-induced tension as a function of web tension, nip force and paper properties

The influence of the winding parameters nip load and web tension on the nip-induced tension shows for all paper types qualitatively the same dependencies:

- The nip-induced tension increases with increasing nip load.
- The nip-induced tension decreases with increasing web tension.

In Table 4 one can find the results of the corresponding experimental series.

Fig. 14 compares the development of the tangential displacement for the 5 tested paper types by applying equal nip load (T_N = 154 N/cm) and web tensions (T_E = 3,0 N/cm). There are differences in the progression of the curves and in the final value of tangential displacement. Paper 6 (WF) has already reached its maximum value after passing 4 times the nip, while the other papers need up to 10 nip passages for building up the final nip-induced tension. The two coated papers 3 and 5 show the highest amount of tangential displacement. If one tries to correlate the observed differences to individual material properties of the papers, one does not see any strong dependencies. The nip-induced mechanism seems to be influenced by a combination of material properties like stress-strain-behaviour in MD and ZD, paper thickness and coefficients of friction.

CONCLUSIONS

A new method to observe the process of building up nip-induced tension in the outer layers of a roll has been presented. It has been shown that the two-dimensional displacement field of the outer layers can be precisely registered with the use of digital image processing. Continuing with experimental investigations, it will be possible to study the quantitative influence of the different parameters involved in the nip mechanics, like the material properties of the web, the process parameters and the machine parameters (e.g. the influence of a compliant roll). Thus it will be possible to achieve a better understanding of the process in the nip.

BIBLIOGRAPHIC REFERENCES

1 K. G. Frey, "Winding", Tappi, Atlanta, 1990, pp. 5-34

2 R. D. Smith (Editor), "Roll and Web Defect Terminology", Tappi, Atlanta, 1995, pp.1-85

3 J. D. Pfeiffer, "Mechanics of a Rolling Nip on Paper Webs", Tappi Journal, Vol. 51, No. 8, 1968, pp. 77A-85A

4 J.K. Good, Z. Wu, "The Mechanism of Nip-Induced Tension in Wound Rolls", Journal of Applied Mechanics, Vol. 60, No.12, 1993, pp.942-947

5 E.G. Welp and B. Gueldenberg, "Analysis of the Kinematic and Dynamic Process During Winding Based on a Systematology of Models for Winding Mechanics", Proceedings of the 4th International Conference on Web Handling, 1997, pp. 71-89

6 J.D. Pfeiffer, "Nip Forces and Their Effect on Wound-in Tension, Tappi Journal, Vol. 60, No. 2, 1977, pp. 115-117

7 J.D. Pfeiffer, "Instrumenting Rolling Nips for Video Recording and Strain Recording", Proceedings of the 2nd International Conference on Web Handling, 1993

8 R. Rand, L. Eriksson, "Physical Properties of Newsprint Rolls During Winding", Tappi Journal, Vol. 56, No. 6, 1973, pp. 153-156

9 R. G. Lucas, "Winder Crepe Wrinkles - Their Causes And Cures", Proceedings of the Tappi Paper Finishing And Converting Conference, 1981, pp. 91-98

10 E.G. Welp and H. Schönmeier, "Untersuchungen zur Verbesserung des Wickelaufbaus in Rollmaschinen", Das Papier, Vol. 37, No. 10A, 1983, pp.V179-V188

11 J. D. McDonald and A. Menard, "Layer-To-Layer Slippage within Paper Rolls During Winding", Proceedings of the 4th International Conference on Web Handling, 1997, pp. 11-25

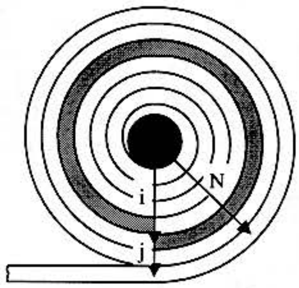

i = 0...N	Number of the observed layer
j = 0...N-i	Number of outer layers relative to layer i
N = i+j(i)	Number of the outermost layer

Fig. 1 Definition of variables

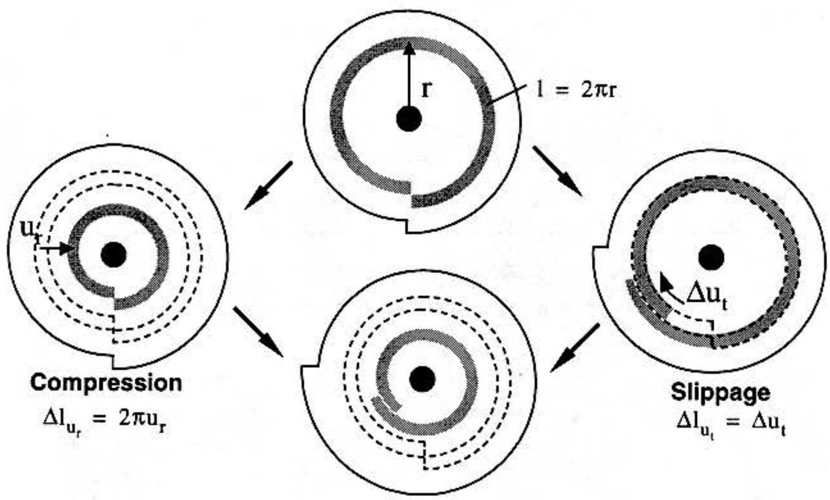

$$\Delta \varepsilon_t = \frac{\Delta l_{u_r} + \Delta l_{u_t}}{l} = \frac{(2\pi u_r + \Delta u_t)}{2\pi r}$$

Fig. 2 Influence of radial and tangential movement on tangential tension

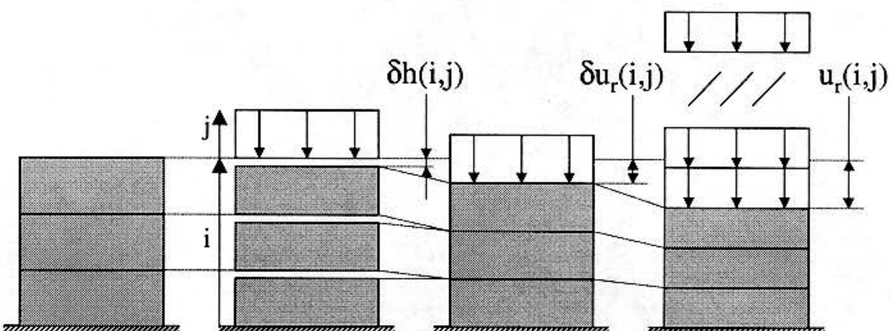

$$\delta h = h \cdot \delta \varepsilon r = h \cdot \frac{\delta \sigma_r}{E} \qquad \delta u_r = \sum_i \delta h \qquad u_r = \sum_j \delta u_r$$

Fig. 3 Radial movement u_r of a layer i in a roll during winding

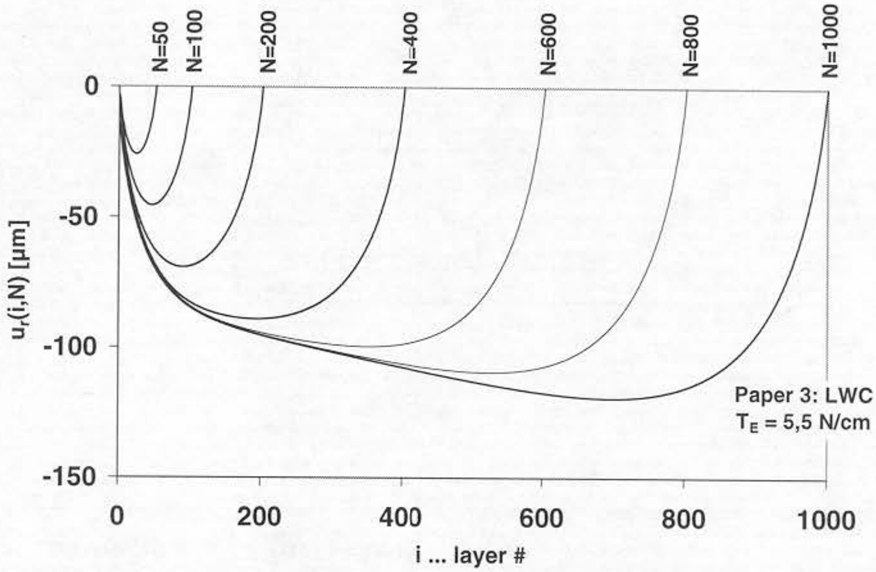

Fig. 4 Example of the radial movement u_r as a function of i (layer #) and N (# of the outermost layer)

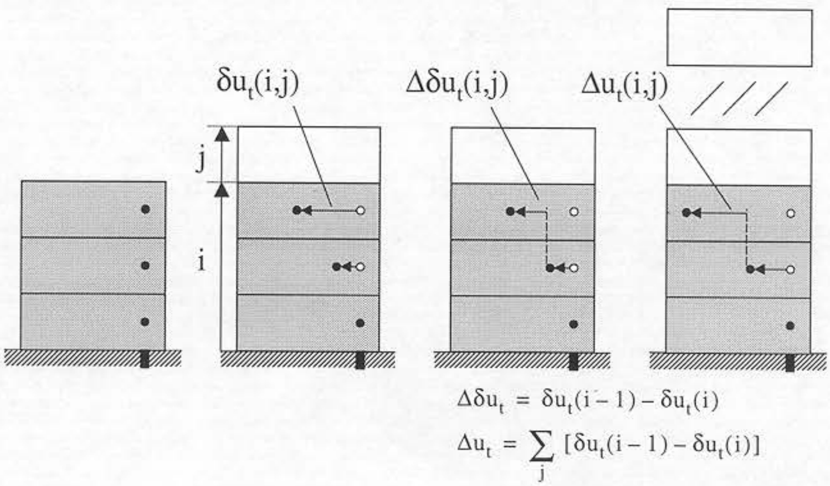

Fig. 5 Tangential movement Δu_t of a layer i during winding

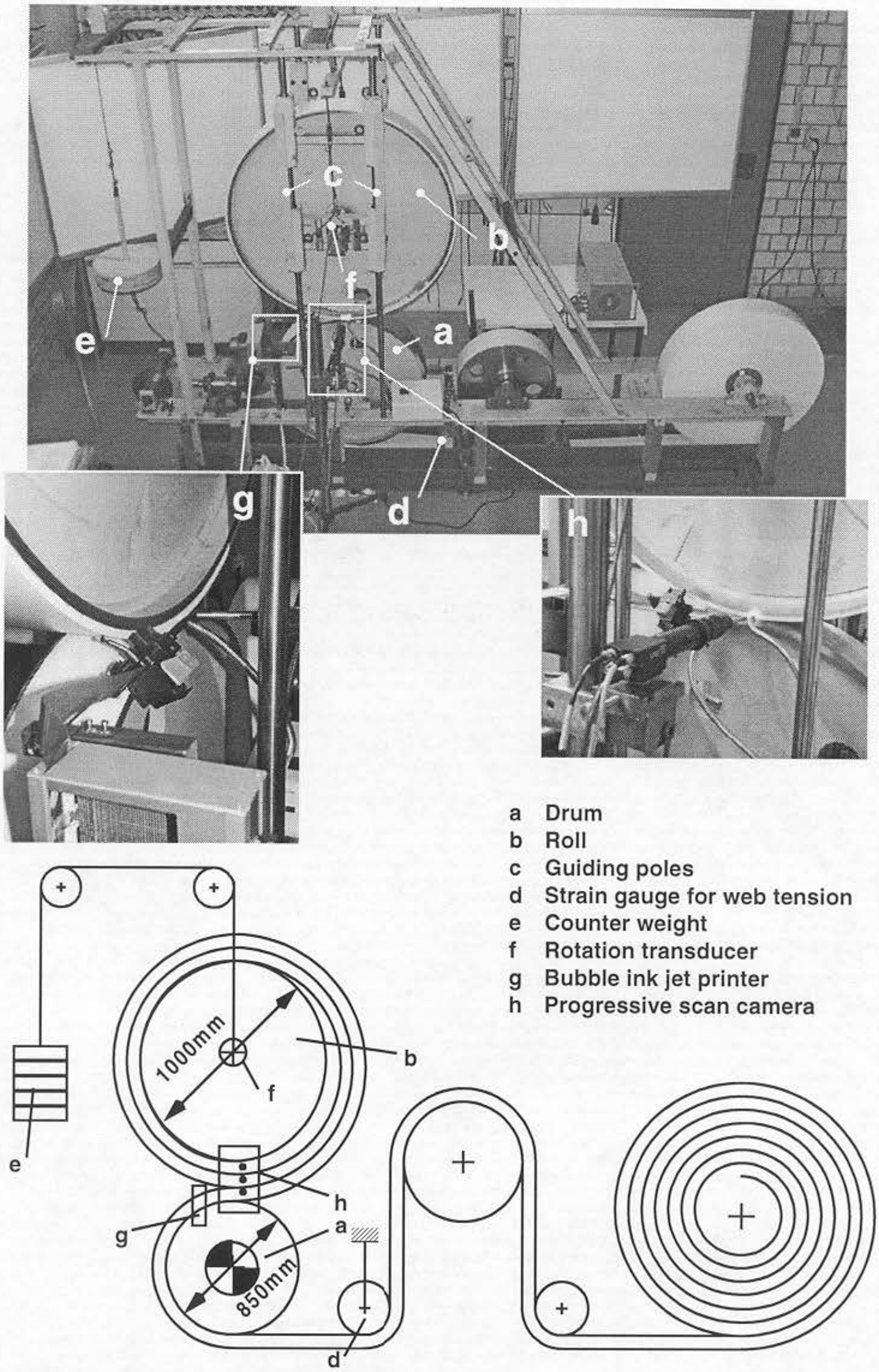

Fig. 6 Experimental winding line

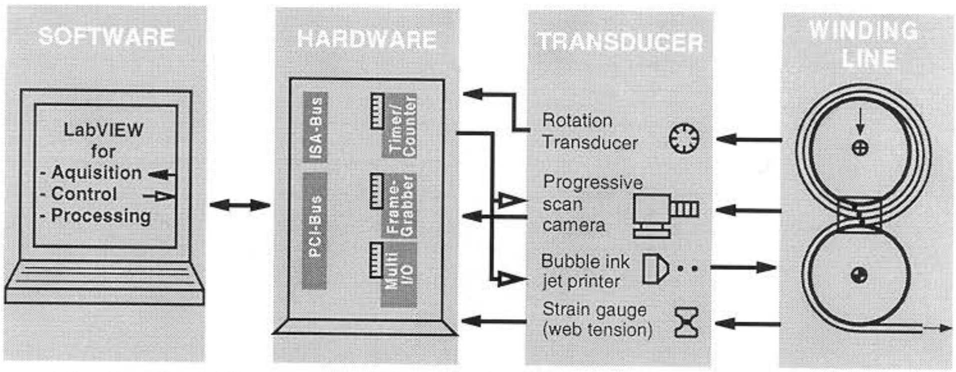

Fig. 7 Aquisition and control system for the experimental winding line

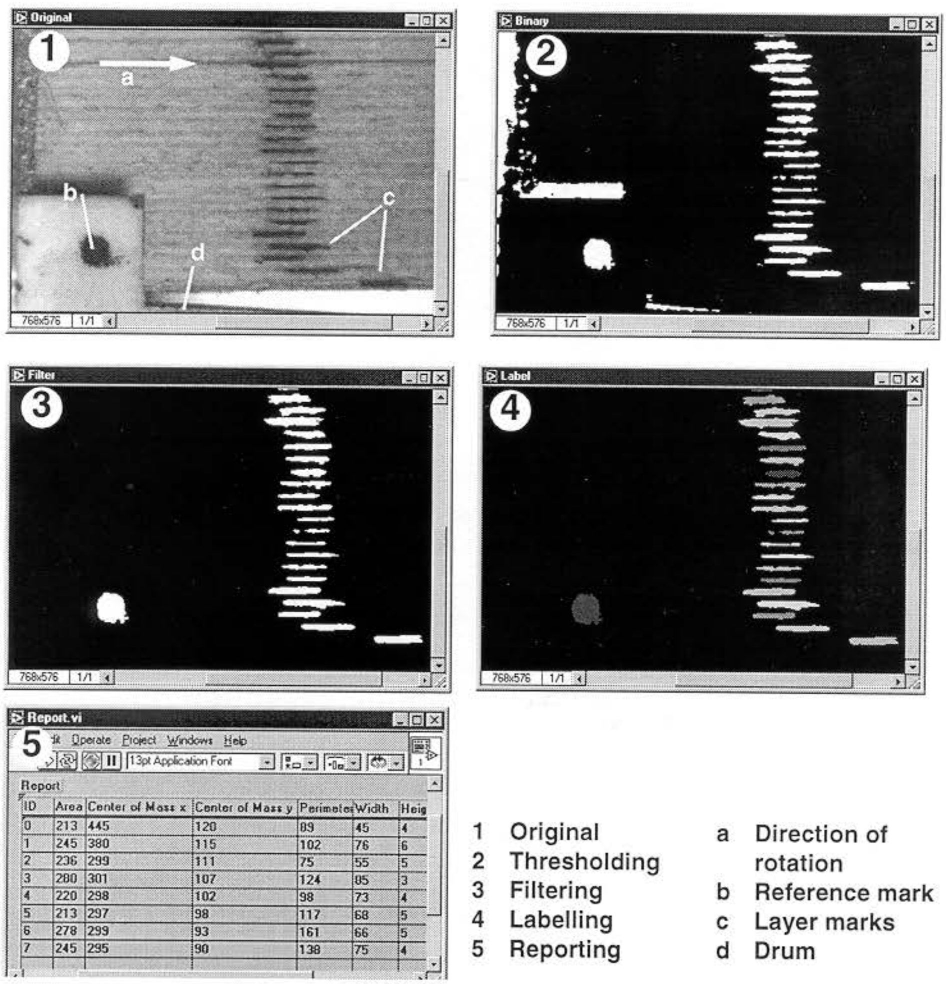

Fig. 8 Image processing

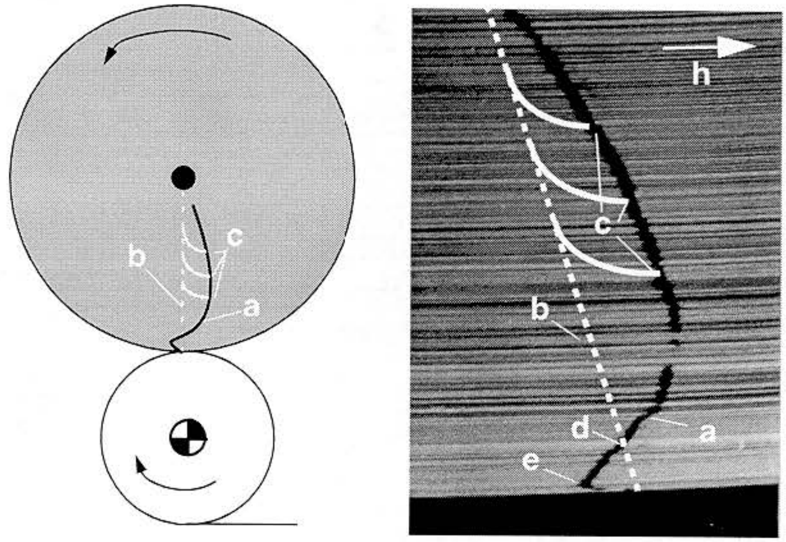

a Layer marks, indicating the total tangential displacement u_t
b Reference line (= position of layer marks in case of $u_t = 0$)
c Direction of rotation
d Layer with displacement $u_t = 0$
e Layer with max. displacement against the direction of rotion
h Direction of rotation

Fig. 9 Picture of the total layer-displacement in a roll taken by experiment

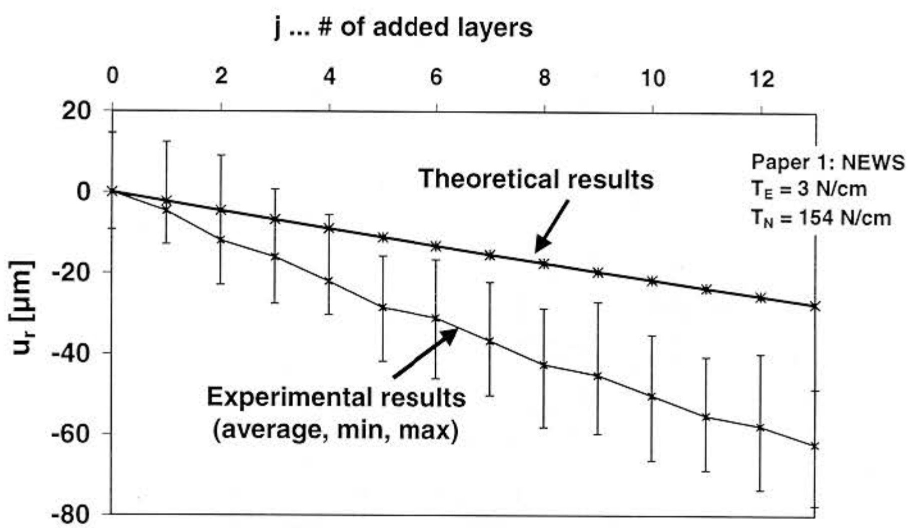

Fig. 10 Comparision of theoretical and experimental results concerning the radial displacement u_r in the outer layers of a roll

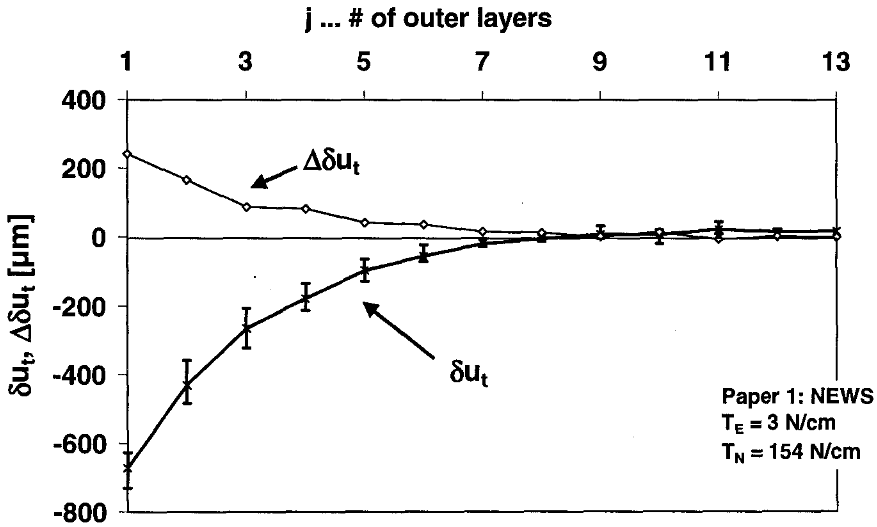

Fig. 11 Experimental results of the tangential displacement δu_t, $\Delta\delta u_t$ in the outer layers of a roll

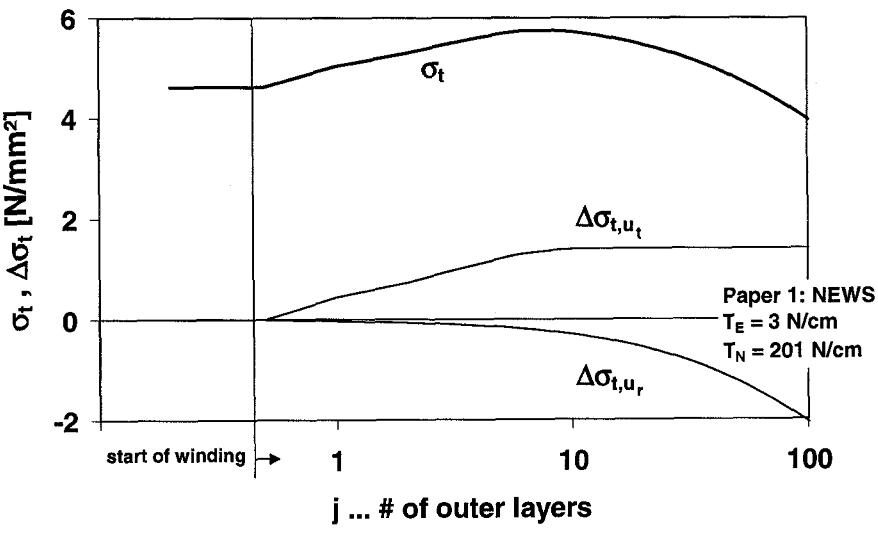

Fig. 12 Development of the total tangential stress in a single layer during the winding process

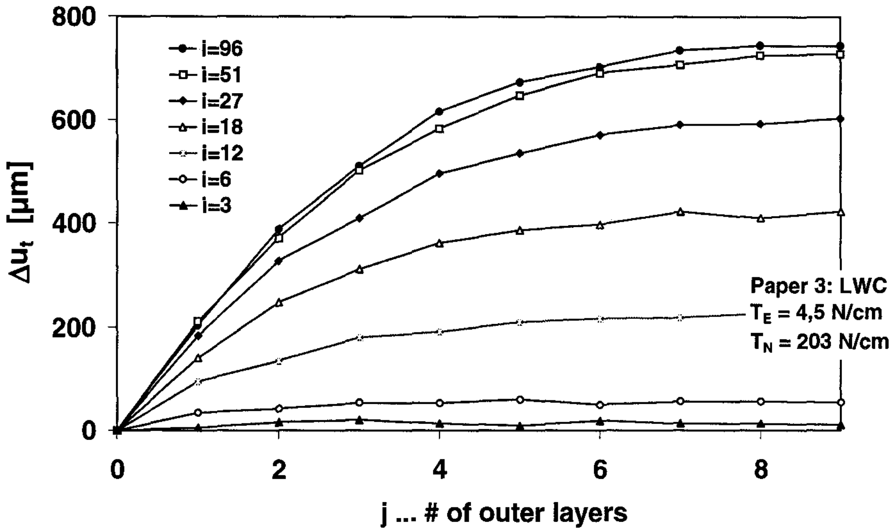

Fig. 13 Tangential displacement Δu_t for different distances from the core (described by layer # i)

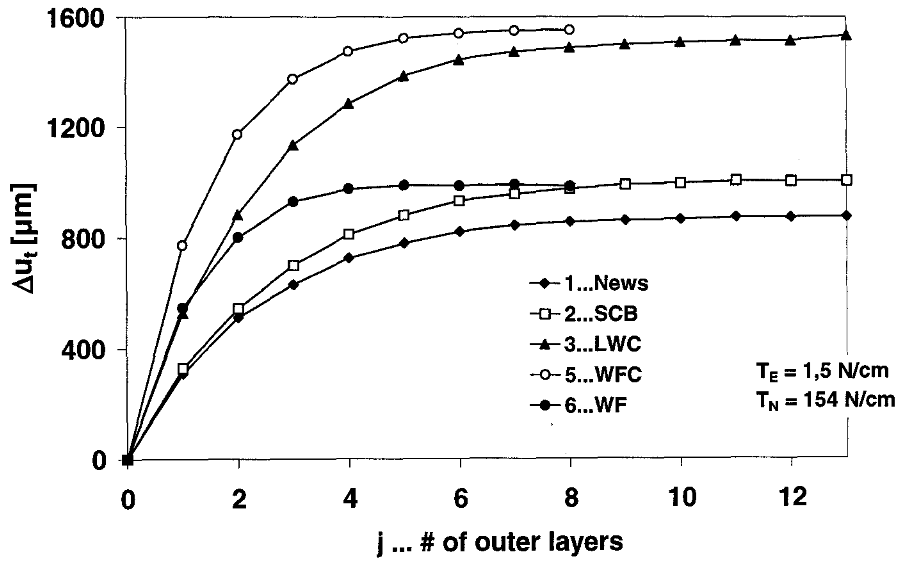

Fig. 14 Tangential displacement Δu_t for different paper grades

Table 1 Material properties of the paper used for experiments

Paper: ID		1	2	3	5	6
Grade		NEWS	SCB	LWC	WFC	WF
Grammage	[g/m²]	45	56	80	100	100
Thickness	[µm]	65,0	50,1	43,2	73,5	121,9
Coefficient of friction:						
Sticking:						
Paper-paper	[-]	0,487	0,568	0,190	0,451	0,613
Steel-paper	[-]	0,126	0,158	0,171	0,231	0,158
Slipping:						
Paper-paper	[-]	0,434	0,487	0,133	0,286	0,575
Steel-paper	[-]	0,107	0,118	0,133	0,173	0,125
E_t (tangential)	[N/mm²]	4400	6500	8500	9300	6100
E_r (radial)						
K1	[-]	0,0360	0,0150	0,0228	0,0140	0,0290
K2	[N/mm²]	24,9	55,8	45,6	201,5	52,6

Table 2 Radial displacement $u_r(i,j=15)$ [µm] calculated by Hakiels winding model

Paper: ID	1		2		3		5		6	
Grade	NEWS		SCB		LWC		WFC		WF	
Web tension T_E [N/cm]	1,5	5,5	1,5	5,5	1,5	5,5	1,5	5,5	1,5	5,5
Layer-#:										
i=50	20	49	14	26	12	25	6	12	11	32
i=100	20	53	15	29	13	28	7	13	12	34
i=200	21	55	15	31	13	29	7	14	13	36
i=500	23	59	16	33	14	31	7	15	15	41
i=1000	25	64	17	35	15	33	8	16	17	46

Table 3 Radial displacement $u_r(j=15)$ [μm] recorded by experiments

Paper: ID	1	2	3	5	6
Grade	NEWS	SCB	LWC	WFC	WF
T_E [N/cm]	1,5-5,5	1,5-5,5	1,5-5,5	1,5-5,5	1,5-5,5
σ_{tE} [N/mm²]	2,3-8,5	3,0-11,0	3,5-12,7	2,0-7,5	1,2-4,5
Average of u_r	74	30		5	27
in different	64	24		4	27
series of	60	31		17	24
experiments	62	33		17	30
	67	22		3	
$\Delta\sigma_{t,u_r}$ [N/mm²]	0,26-0,33	0,14-0,21		0,03-0,16	0,15-0,18

Table 4 Nip-induced stress $\Delta\sigma_{t,u_t}$ as a function of nip load T_N and incoming web tension T_E

Paper 2: LWC			
T_E = 3 N/cm, T_N [N/cm]:	105	154	203
$\Delta\sigma_{t,u_t}$ [N/mm²]	0,80	1,21	1,40
T_N = 154 N/cm, T_E [N/cm]:	1,5	3,0	5,5
$\Delta\sigma_{t,u_t}$ [N/mm²]	1,97	1,21	0,74
Paper 5: WFC			
T_E = 3 N/cm, T_N [N/cm]:	105	154	203
$\Delta\sigma_{t,u_t}$ [N/mm²]	2,02	3,02	3,84
T_N = 154 N/cm, T_E [N/cm]:	1,5	3,0	5,5
$\Delta\sigma_{t,u_t}$ [N/mm²]	4,40	3,02	2,00

B. Gueldenberg And E. G. Welp
Quantitative Analysis of Nip-Induced Tension by Use of Image Processing
6/7/99 Session 1 9:20 – 9:45 a.m.

Question - Ron Swanson, 3M
Very impressed and interested in your analysis. Have you or how did you account for the ink jet not being right on the net delay there and the delay for the actual ink time of flight?

Answer - B. Gueldenberg, Ruhr University
As you have seen in one picture, which is shown here again (Fig. 9), we have to account for that delay caused by the position of the ink jet cartridge in front of the nip. Then is a certain length of paper between the position of the cartridge and the middle of the nip. This length remains constant, while the diameter of the roll is always increasing. For the case of no slippage, the printed line has a small angle in the direction of rotation. However, due to the fact that we have to determine differences of the displacement of two neighboring layers when calculating the stress and strain changes, this delay doesn't have any effect on the results. The delay occurs for both layers marks in a very similar way.

Questions - David Pfeiffer, JDP Innovations Inc.
I am very reassured by your findings that you are actual proving what I had only conjectured for many years and it's remarkable that you can do this kind of work. I was really out on the limb many times explaining J-lines to people with the suspected mechanism that now I see that you have confirmed this and the spectacular work on newsprint winding shows the kind of mechanism that I thought was probably responsible for causing crepe wrinkles. And you have seen it and put the finger on it. So it is remarkable work and I think you should be congratulated for it.